

# Biophysical properties of tear film lipid layer I. Surface tension and surface rheology

Xiaojie Xu,<sup>1</sup> Guangle Li,<sup>1</sup> and Yi Y. Zuo<sup>1,2,\*</sup>

<sup>1</sup>Department of Mechanical Engineering, University of Hawaii at Manoa, Honolulu and <sup>2</sup>Department of Pediatrics, John A. Burns School of Medicine, University of Hawaii, Honolulu

**ABSTRACT** Tear film lipid layer (TFLL) is the outmost layer of the tear film. It plays a crucial role in stabilizing the tear film by reducing surface tension and retarding evaporation of the aqueous layer. Dysfunction of the TFLL leads to dysfunctional tear syndrome, with dry eye disease (DED) being the most prevalent eye disease, affecting 10%–30% of the world population. To date, except for treatments alleviating dry eye symptoms, effective therapeutic interventions in treating DED are still lacking. Therefore, there is an urgent need to understand the biophysical properties of the TFLL with the long-term goal to develop translational solutions in effectively managing DED. Here, we studied the composition-function correlations of an artificial TFLL, under physiologically relevant conditions, using a novel experimental methodology called constrained drop surfactometry. This artificial TFLL was composed of 40% behenyl oleate and 40% cholesteryl oleate, representing the most abundant wax ester and cholesteryl ester in the natural TFLL, respectively, and 15% phosphatidylcholine and 5% palmitic-acid-9-hydroxy-stearic-acid (PAHSA), which represent the two predominant polar lipid classes in the natural TFLL. Our study suggests that the major biophysical function of phospholipids in the TFLL is to reduce the surface tension, whereas the primary function of PAHSA is to optimize the rheological properties of the TFLL. These findings have novel implications in better understanding the physiological and biophysical functions of the TFLL and may offer new translational insight to the treatment of DED.

**SIGNIFICANCE** Tear film lipid layer (TFLL) stabilizes the tear film by reducing surface tension and retarding evaporation of the aqueous layer. Dysfunction of the TFLL leads to the dry eye disease that affects 10%–30% of the world population. To date, surface and rheological properties of the TFLL are still poorly understood. Here we studied the composition-function correlations of an artificial TFLL, under physiologically relevant conditions, using a novel experimental methodology called constrained drop surfactometry. We have concluded that the major biophysical function of phospholipids in the TFLL is to reduce the surface tension, whereas the primary function of fatty acid esters of hydroxy fatty acids is to optimize the rheological properties of the TFLL.

## INTRODUCTION

Tear film is a multilayered biological barrier that protects our eyes from potential risks from the environment (1,2). The thickness of a normal tear film is 6–10  $\mu\text{m}$  (3). As shown in Fig. 1 a, it is composed of three consecutive layers, i.e., the inner mucin layer, the intermediate aqueous layer, and the outermost lipid layer (4). The mucin layer mainly consists of sugar-rich glycosylated proteins that function as lubricants to facilitate spreading of the tear film at the ocular surface (5). The aqueous layer, representing the

largest portion of the tear film with a thickness of approximately 4  $\mu\text{m}$ , is made of solutions of electrolytes, peptides, and proteins (6).

The lipid layer, commonly known as the tear film lipid layer (TFLL), is approximately 40 nm thick (7). It consists of two sublayers, i.e., a polar lipid layer adjacent to the aqueous layer and a nonpolar lipid layer that resides upon the polar lipids and is directly exposed to air (4,8). The polar lipids account for 20 mol% of the TFLL, with phospholipids being the most abundant lipid class ( $\sim 12$  mol%) in human tears (9). A recent lipidomics study identified a new class of polar lipids, (O-acyl)- $\omega$ -hydroxy fatty acids (OAHFAs), accounting for  $\sim 4$  mol% of the TFLL (8,10–12). The nonpolar lipids account for 80 mol% of the TFLL, with wax esters (WEs, i.e., esters of a fatty acid and a fatty alcohol, accounting for  $\sim 43$  mol%) and cholesteryl esters

Submitted August 14, 2021, and accepted for publication December 22, 2021.

\*Correspondence: [yzuo@hawaii.edu](mailto:yzuo@hawaii.edu)

Editor: John Conboy.

<https://doi.org/10.1016/j.bpj.2021.12.033>

© 2021 Biophysical Society.



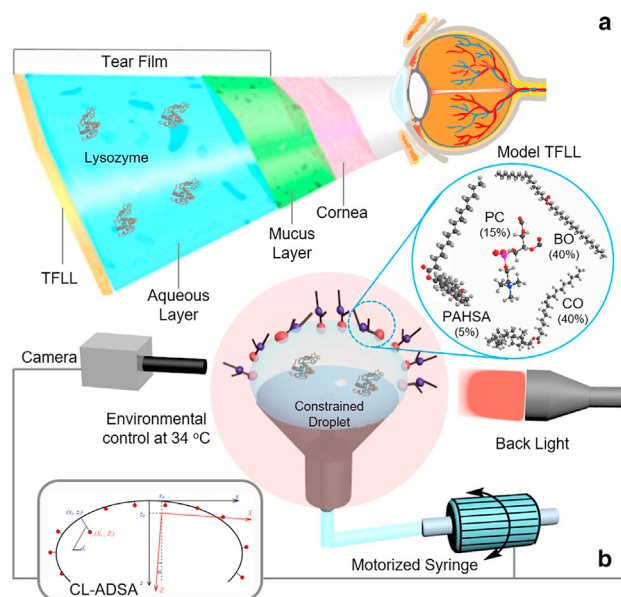


**FIGURE 1** Schematics of (a) the tear film and (b) the constrained drop surfactometry (CDS) for biophysical simulations of the tear film lipid layer (TFL). CDS uses the air-water surface of a sessile drop ( $\sim 4$  mm in diameter,  $\sim 0.3$  cm<sup>2</sup> in surface area, and  $\sim 20$   $\mu$ L in volume), constrained on a carefully machined pedestal with knife-sharp edges, to accommodate the spread TFL. The buffer droplet, simulating the chemical compositions of the tear film aqueous layer, is enclosed in an environmental control chamber that maintains the physiologically relevant temperature of 34°C. The model TFL consists of BO:CO:PC:PAHSA (40:40:15:5). The TFL is compressed and expanded at a highly dynamic rate of 15% relative area per second to simulate a blink, by regulating fluid flow into and out of the droplet using a motorized syringe. Dynamic surface tension of the TFL is determined with closed-loop axisymmetric drop shape analysis (CL-ADSA), which measures surface tension of the TFL remotely by analyzing the shape of the TFL-covered droplet in real-time using photographic methods.

(CEs, i.e., esters of a fatty acid and a cholesterol, accounting for  $\sim 39$  mol%) being the most prevalent nonpolar lipid classes (13).

It is believed that the major physiological function of the TFL is to stabilize the tear film by reducing surface tension and retarding evaporation of the aqueous layer (11,14–16). Dysfunction of the TFL leads to dysfunctional tear syndrome (17,18), with dry eye disease (DED) being the most prevalent eye disease, affecting 10%–30% of the world population (19). DED is a multifactorial ocular disease characterized by damage of corneal epithelia, inflammation of ocular surface, eye discomfort, and visual disturbance, as a result of compromised tear film stability (20,21). To date, except for treatments alleviating dry eye symptoms, effective therapeutic interventions in treating DED are still lacking (22). It is estimated that DED directly and indirectly causes a \$55 billion annual economic burden in the United States alone (23). Therefore, there is an urgent need to understand the biophysical properties of the TFL and to develop translational solutions in effectively managing the DED.

There have been many *in vitro* studies that have investigated the surface activities of either artificial TFL (24–26) or meibomian lipids extracted from either human (27) or animal sources (28). Although providing valuable biophysical and physiological insights, these studies have a few common limitations. First of all, lipid composition of the artificial TFL used in most previous studies deviated significantly from that of the natural TFL. Polar lipids, mainly phosphatidylcholine (PC), have been commonly used *in vitro* to constitute the artificial TFL (29). However, PC accounts for less than 20 mol% of the natural TFL, whereas the other 80 mol% of the natural TFL is composed of nonpolar lipids (15,30). This discrepancy is revealed by the rapid development of lipidomics in recent years, which allows comprehensive lipid analysis of meibomian gland secretions and discovery of never-before-known lipid classes, such as OAH-FAs (8,10,31), whose biophysical function and contribution to the TFL are still poorly understood.

In addition, the experimental conditions used in most previous *in vitro* studies can hardly mimic the physiological conditions of the ocular surface and/or the dynamics of the TFL. This limitation is largely due to existing *in vitro* biophysical methods used for studying the TFL. These methods include the Langmuir trough (24–28,32–35), capillary tube (36), pendent drop (37), sessile drop and bubble (38,39). Among these methods, the Langmuir trough is the most commonly used method for studying the TFL. However, Langmuir trough has a few limitations that prevent it from mimicking the physiological conditions of the ocular surface and the dynamics of the TFL. First, due to its large size, the Langmuir trough generally lacks rigorous temperature control. Hence most Langmuir trough experiments were conducted at room temperature. However, the ocular surface is estimated to have a physiological temperature of 34°C (27,40). Second, the Langmuir trough is incapable of simulating the physiologically relevant tear film dynamics. The tear film is spread and replenished at the ocular surface, compressed and expanded rapidly during each individual blink. A healthy adult blinks approximately 10 times per minute with an average duration of 0.1–0.3 s per blink (41). It means that the TFL must undergo highly dynamic compression (during the closing phase of the blink) and expansion (during the opening phase of the blink) (42). Langmuir trough is unable to perform fast compression and expansion as doing so generates waves that disturb the surface tension measurements by the Wilhelmy plate (43). Third, it is difficult, if not impossible, for the Langmuir trough to study the effect of biological ligands in the aqueous layer of the tear film. The aqueous layer contains electrolytes, peptides, and proteins, mainly lipocalin (44), lysozyme (45), and lactoferrin (46). It is not unexpected that these ligands interact with the TFL during normal physiological conditions. However, the Langmuir trough commonly requires a large aqueous subphase of at least 100 mL, which complicated the study of surface interaction

and molecular recognition between the TFLL and biological ligands in the aqueous layer.

Here, we studied the biophysical properties of an artificial TFLL using a novel experimental methodology called constrained drop surfactometry (CDS). CDS is a new generation of droplet-based surface tensiometry that we developed initially for studying the biophysical properties of pulmonary surfactant films (47,48). We have shown that CDS is superior to previous *in vitro* methods in permitting high-fidelity biophysical simulations of pulmonary surfactant films by precisely controlling the physiologically relevant experimental conditions, such as core body temperature, highly dynamic compression and expansion cycles, and adsorption from high surfactant concentrations (49–51). Given the biophysical similarities between the pulmonary surfactant film and the TFLL (52), we hypothesize that CDS would be an ideal *in vitro* model for biophysical simulations of the TFLL. Using CDS, we have systematically studied the surface properties of various tear lipid films (TLFs) closely relevant to the natural TFLL. These TLFs are behenyl oleate (BO) and cholesteryl oleate (CO), representing the most abundant WE and CE in the TFLL, respectively (53). Phosphatidylcholine (PC) and palmitic-acid-9-hydroxy-stearic-acid (PAHSA) represent the two predominant polar lipid classes in the TFLL. It should be noted that the chemical composition of this artificial TFLL has two major limitations when comparing to natural TFLL. First, human meibomian lipids are composed of a complex mixture of different lipid classes, including mainly WEs, CEs, OAHFAs, cholesteryl esters of OAHFA, phospholipids, sphingomyelins, free fatty acids, sterols, triacylglycerols, and a small amount of other polar and nonpolar lipids (1). Each of these lipid classes consists of many homologous lipid species varying in lengths, degrees of unsaturation, and branching, which is essential for the natural TFLL to have proper melting and lipid mixing (54). Hence, the artificial TFLL studied here, consisting of only four lipid classes of the natural TFLL, is an overly simplified model, which is designed to understand the composition-function correlations of major lipid classes in the TFLL. Second, PAHSA and OAHFAs both belong to a structurally similar general class of lipids named fatty acid esters of hydroxy fatty acids (FAHFAs), which are lipids consisting of two acyl chains connected through a single ester bond (31). However, OAHFAs differ from PAHSA in the length of their hydroxy fatty acids, degree of saturation, and the location of the hydroxy esterification. Hence, PAHSA was only used as a remote model of OAHFAs, since the structural similarity shared by these two lipids could result in comparable surface activities.

Our data suggest distinctive composition-function correlations for the lipid components in the artificial TFLL. Although the major biophysical function of phospholipids in the TFLL is to reduce the surface tension, the primary function of FAHFAs is to optimize the surface rheological properties of the TFLL. These findings have novel implications in better understanding the physiological and biophys-

ical functions of the TFLL and may offer new translational insight in the treatment of DED.

## MATERIALS AND METHODS

### Materials

L- $\alpha$ -phosphatidylcholine (PC) from egg yolk, palmitic-acid-9-hydroxy-stearic-acid (PAHSA), BO, and CO were purchased and used without further purification. Physicochemical properties, chemical structures, and sources of these lipids are summarized in Table 1. Individual lipids were dissolved in chloroform as 1 mM stock solutions. Lysozyme, being a major protein found in the aqueous layer of the tear film (33), was purchased from Sigma-Aldrich. Phosphate-buffered saline (PBS) was purchased from Fisher Scientific. Water used was Milli-Q ultrapure water with a resistivity greater than 18 M $\Omega$ ·cm at room temperature.

### Constrained drop surfactometry

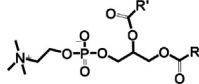
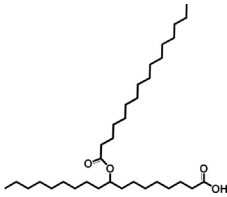
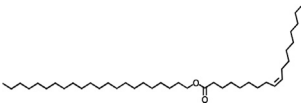
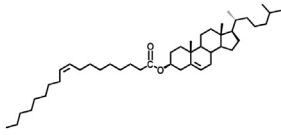
CDS is a new generation of droplet-based surface tensiometry technique developed in our laboratory (47,48). It uses the air-water surface of a sessile drop ( $\sim 4$  mm in diameter,  $\sim 0.3$  cm<sup>2</sup> in surface area, and  $\sim 20$   $\mu$ L in volume) to accommodate the spread or adsorbed film. As shown in Fig. 1 *b*, a key design of the CDS is a carefully machined pedestal that uses its knife-sharp edge to prevent film leakage even at very low surface tensions. System miniaturization of the CDS facilitates rigorous control of the experimental conditions with an environmental control chamber. The spread and adsorbed film at the droplet surface can be compressed and expanded by precisely controlling oscillation of the surface area of the droplet using a newly developed mechatronic system called closed-loop axisymmetric drop shape analysis (CL-ADSA) (55). CL-ADSA determines the surface tension of the spread and adsorbed film by analyzing the shape of the film-covered droplet. The surface pressure ( $\pi$ ) can be determined from the surface tension ( $\gamma$ ) using  $\pi = \gamma_0 - \gamma$ , with  $\gamma_0$  being the surface tension of a clean, surfactant-free air-water surface.

Approximately 0.06  $\mu$ g lipid samples, i.e., 0.1  $\mu$ L at a lipid concentration of 1 mM, were spread onto the air-water surface of a droplet (with a surface area of  $\sim 0.6$  cm<sup>2</sup>) that works as an aqueous subphase to the TFLL. Hence, the initial surface density of the lipids before the monolayer compression was 0.1  $\mu$ g/cm<sup>2</sup>, corresponding to a molecular area of  $\sim 100$   $\text{\AA}^2$ /molecule. To study the effect of chemicals in the subphase, the droplet was switched among the pure water, saline, PBS, or 1 mM lysozyme solution, respectively. The spread film was left undisturbed for 1 min to allow evaporation of solvent. The droplet was then slowly expanded to decrease the surface pressure to around zero (i.e., increasing the surface tension to around 70 mN/m). Subsequently, the spread lipid film was compressed and expanded at two extreme rates, i.e., 0.15 and 15 relative area per second (A%/s), and at two different environmental temperatures, i.e., 20°C and 34°C, respectively.

The TFLL spread on the ocular surface of human eyes has an approximate surface area of 1–3 cm<sup>2</sup> (56), which is only three to ten times larger than the surface area of the sessile drop used in CDS (i.e.,  $\sim 0.3$  cm<sup>2</sup>). Given the maximum eyelid speeds in the range of 0.1–0.3 m/s and the time period of a typical unforced blink at 0.3 s (57), the film compression rate of the TFLL during a typical blink is estimated at approximately 10 cm<sup>2</sup>/s. The high compression rates of 15 A%/s used in our experiments corresponds to 0.045 cm<sup>2</sup>/s, which is still 200 times slower than the actual blinking process. Nevertheless, the compression rate of 15 A%/s used in our experiments is significantly higher than the maximum possible compression rate of a Langmuir trough. This high compression rate is used to study the kinematic effect of TFLL under physiologically relevant conditions, in comparison to quasi-static compressions at the rate of 0.15 A%/s.

The lipid film was compressed and expanded for at least five cycles. Usually after the first cycle, the compression and expansion isotherms became repeatable. The fifth cycle was investigated as representative of the surface

**TABLE 1** Lipids studied in the biophysical simulations of the tear lipid films

Lipid	Chemical Formula	Chemical Structure	Chemical Supplier	Purity	Molecular Weight (g/mol)	Melting Temperature
L- $\alpha$ -phosphatidylcholine (PC)	C16:0 (33%), C18:1 (32%), C18:2 (17%), C18:0 (12%), Others (6%)		Sigma-Aldrich	99%	~770	-15 to about -7°C
Palmitic-acid-9-hydroxy-stearic-acid (PAHSA)	C <sub>34</sub> H <sub>66</sub> O <sub>4</sub> (C18:0-C16:0)		Sigma-Aldrich	95%	539	33.5°C
Behenyl oleate (BO)	C <sub>40</sub> H <sub>78</sub> O <sub>2</sub> (C22:0-C18:1)		Larodan	99%	591	38°C
Cholesteryl oleate (CO)	C <sub>45</sub> H <sub>78</sub> O <sub>2</sub> (cholesterol-C18:1)		Sigma-Aldrich	98%	651	44-47°C

activity of lipid films. Surface activity of the lipid films was quantified with the maximum surface pressure ( $\pi_{\max}$ ) reached at the end of film compression, and the average film compressibility  $\kappa = \frac{1}{A} \frac{\partial A}{\partial \gamma}$ . It should be noted that the actual biomechanics of blinking is much more complicated than simply oscillating the surface area of the TFLL. Each blink is accompanied by a lipid replenishment from the meibomian glands and the tear meniscus, which constantly changes the thickness, and possibly, composition of the TFLL.

### Surface dilational rheology

Detailed experimental protocols for determining the surface dilational modulus  $E = \frac{d\gamma}{dlnA}$  of the lipid films using CDS can be found elsewhere (58,59). Briefly, surface area of the spread lipid films was oscillated in a sinusoidal waveform, with a series of predefined frequencies (0.025, 0.05, 0.1, 0.25, 0.5, and 1 Hz) using CL-ADSA. The amplitude of area oscillation was limited to 10% of the initial surface area to minimize nonlinear effects. The surface tension response to the surface area oscillation was recorded as the output and was compared against the surface area oscillation waveform as the input. The elastic ( $E_r$ ) and viscous ( $E_i$ ) components of the surface dilational modulus were determined from the phase shift ( $\varphi$ ) between the input and output waveforms, and from the oscillation amplitudes of the surface area and the surface tension. The loss tangent ( $\tan\varphi$ ) was calculated as the ratio between the viscous modulus and the elastic modulus ( $E_i/E_r$ ). All measurements were carried out at  $34 \pm 1^\circ\text{C}$  for at least three times.

### Statistical analysis

All results were shown as mean  $\pm$  standard deviation ( $n > 3$ ). One-way ANOVA with Tukey's means comparison test was used to determine group differences (OriginPro, Northampton, MA). A value  $p < 0.05$  was considered to be statistically significant.

## RESULTS

### Surface activities of the tear lipid films

Fig. 2 shows the compression and expansion isotherms of five characteristic TLFs, at different temperatures (20°C and 34°C) and compression rates (0.15 and 15 A%/s), respectively. These lipid films are two individual polar lipids, i.e., PC and PAHSA, the combined polar lipid films, i.e., PC:PAHSA (3:1), the combined nonpolar lipid film, i.e., BO:CO (1:1), and the recombinant artificial TFLL, i.e., BO:CO:PC:PAHSA (40:40:15:5). Reproducibility of these results can be found in Fig. S1. Pure water was used as the subphase in all of these experiments.

Fig. 2a shows the compression and expansion isotherms of the five TLFs at room temperature with a quasi-static cycling rate of 0.15 A%/s. These results are comparable to those obtained with the Langmuir trough under similar experimental conditions (29,34). To demonstrate the accuracy of our method, Fig. S2 shows the agreement between the compression isotherms of PC obtained with CDS and those obtained with the Langmuir trough at room temperature.

As shown in Fig. 2a, among the two polar lipid films, PC collapses at 46 mN/m; but PAHSA collapses at a much lower surface pressure of only 25 mN/m. The combined polar lipid film, i.e., PC:PAHSA (3:1), shows a similar surface activity as PC. But the compression isotherms shift slightly to the left, indicating gradual squeeze-out of PAHSA from

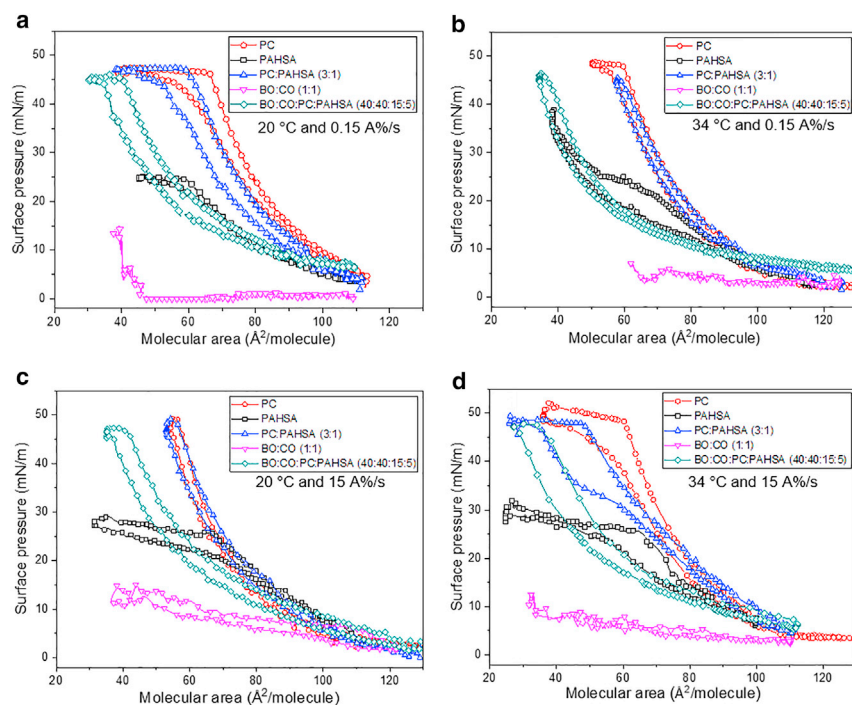


FIGURE 2 Effect of temperature and compression rate on the surface activity of tear lipid films (TLFs). Compression-expansion isotherms of PC, PAHSA, PC:PAHSA (3:1), BO:CO (1:1), and BO:CO:PC:PAHSA (40:40:15:5) at (a) room temperature and a low compression rate (0.15 A%/s), (b) 34°C and the low compression rate (0.15 A%/s), (c) room temperature and a high compression rate (15 A%/s), and (d) the physiologically relevant temperature (34°C) and high compression rate (15 A%/s).

the combined polar lipid film. The combined nonpolar film, i.e., BO:CO (1:1), is nearly infinitely compressible and shows moderate surface pressure increase only at an extreme film compression below  $50 \text{ \AA}^2/\text{molecule}$ . The recombinant TFLL, i.e., BO:CO:PC:PAHSA (40:40:15:5), shows similar isotherm shape and collapse pressure as PC, except for significantly shifting the isotherms to the left. These results indicate that PC plays a predominate role in controlling the surface activity of the TFLL, while the nonpolar lipids are squeezed out from the interfacial monolayer almost instantaneously, and most likely residing atop of the lipid monolayer due to the strong hydrophobicity of these nonpolar lipids.

Fig. 2 b shows the quasi-static compression and expansion isotherms of the five TLFs at 34°C. It is found that increasing temperature to 34°C did not have a significant effect on the lipid films other than PAHSA. This is not unexpected because the melting temperature of PC, i.e.,  $-15^\circ\text{C}$  to about  $-7^\circ\text{C}$ , is much lower than either room temperature or the physiological temperature. However, the melting temperature of PAHSA, i.e.,  $33.5^\circ\text{C}$  (Table 1), is very close to the physiological temperature of the TFLL. Surprisingly, it is found that the surface pressure of PAHSA increases to more than 40 mN/m at 34°C, whereas it collapses at 25 mN/m at room temperature.

Fig. 2 c shows the dynamic compression and expansion isotherms of the five TLFs at room temperature. In comparison to quasi-static processes at the same temperature (Fig. 2 a), both PAHSA and nonpolar lipids show a kinetically driven increase in surface pressure. Fig. 2 d shows the

compression and expansion isotherms of the five TLFs under physiologically relevant conditions, i.e., 34°C and a high compression rate 100 times of that used in the quasi-static process. It is found that all TLFs containing PC collapse at around 50 mN/m. With reducing PC content, the compression isotherms shift to the left. Together with those shown in Fig. 2 a–c, all results indicate that PC, although accounting for only 15% of the artificial TFLL, plays the predominant role in increasing surface pressure (i.e., reducing surface tension) of the TFLL. Another polar lipid, PAHSA, collapses at the surface pressure around 30 mN/m, indicating that the primary biophysical role of PAHSA is not surface tension reduction. The nonpolar lipids are mostly not surface active.

Statistical analyses of the surface activity of the TLFs under various experimental conditions are summarized in Fig. 4 a and b, which shows the maximum surface pressure ( $\pi_{\text{max}}$ ) and film compressibility ( $\kappa$ ), respectively. Since the nonpolar lipid film BO:CO is essentially infinitely compressible, its compressibility is not shown in Fig. 4 b. It can be seen that the  $\pi_{\text{max}}$  of the TFLL is largely determined by PC. Film compressibility ( $\kappa$ ) measures the “hardness” of a two-dimensional material, such as the lipid film. A low  $\kappa$  indicates an incompressible “hard” film, whereas a high  $\kappa$  indicates a “soft” film (43). As shown in Fig. 4 b, among the two polar lipids studied,  $\kappa$  of PC at the physiologically relevant condition is 0.7 m/mN. In comparison,  $\kappa$  of PAHSA appears to be insensitive to the experimental conditions and maintains a nearly constant value of 1.7 m/mN at all temperatures and compression rates. Under the same

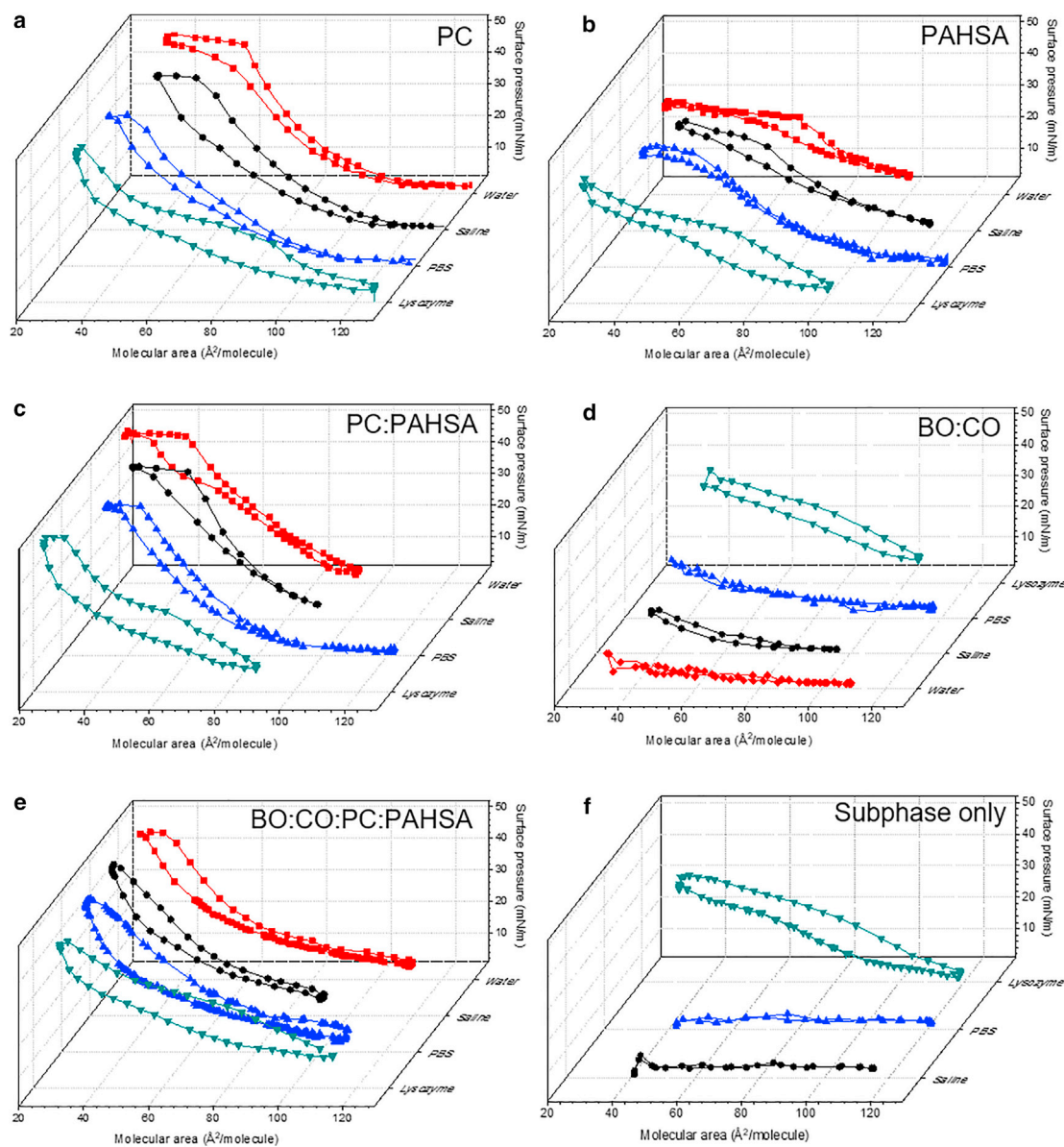


FIGURE 3 Effect of subphase composition on the surface activity of tear lipid films (TLFs). Compression-expansion isotherms of (a) PC, (b) PAHSA, (c) PC:PAHSA (3:1), (d) BO:CO (1:1), (e) BO:CO:PC:PAHSA (40:40:15:5), and (f) subphase alone without TLFs. For each TLF, four subphases with increasing complexity of chemical composition were studied. These were pure water, saline (0.9 wt%), PBS, and the lysozyme solution (1 mM), respectively. All biophysical simulations were conducted at the physiologically relevant temperature (34°C) and high film compression rate (15 A%/s).

experimental condition,  $\kappa$  increases with reducing PC contents of the lipid films. At the physiological relevant condition,  $\kappa$  of PC, PC:PAHSA, and BO:CO:PC:PAHSA gradually increases from 0.7 to 1.4 m/mN. These results indicate that PAHSA, although not contributing to directly decreasing surface tension of the TFL, plays a role in “softening” the TFL by increasing its compressibility.

Fig. 3 shows the effect of four different subphases on the surface activity of the TLFs. These subphases are, with the increasing chemical complexity, pure water, saline (0.9 wt%), PBS, and 1 mM lysozyme solution. All compression and expansion isotherms were obtained at the physiologi-

cally relevant conditions of 34°C and high compression rate. Reproducibility of these isotherms is shown in Fig. S3. Being a control, Fig. 3 f shows the compression and expansion isotherms of the subphases alone, i.e., without TLFs. It is clear that neither saline nor PBS is surface active, but lysozyme demonstrates a moderate surface activity, up to a surface pressure of 34 mN/m at the end of compression.

For the three PC-containing TLFs (Fig. 3 a, c, and e), the effect of subphase on the compression and expansion isotherms is only moderate, except that lysozyme increases the hysteresis of the compression and expansion loop. For

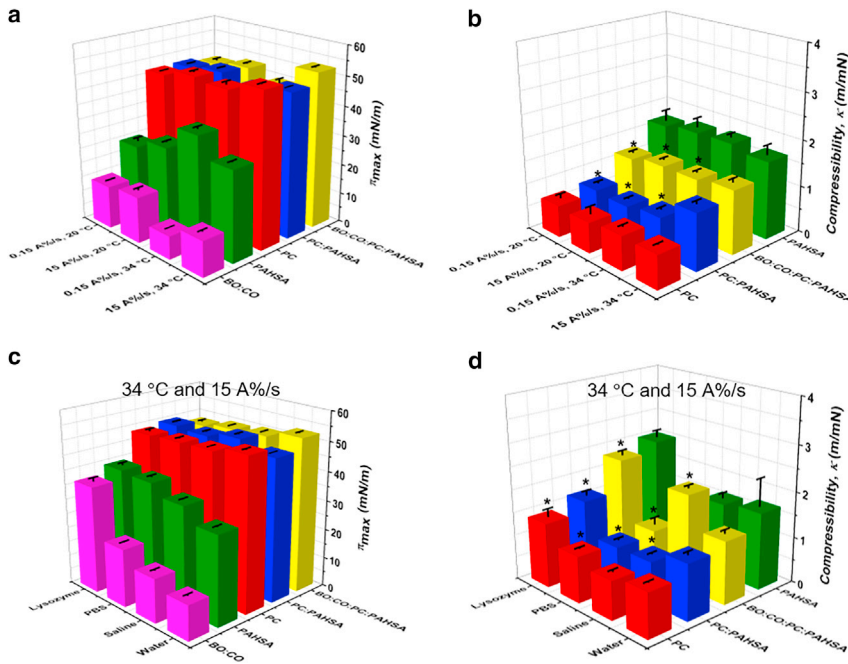


FIGURE 4 Statistical analysis of the surface activity of tear lipid films (TLFs). (a and b) The maximum surface pressure ( $\pi_{\max}$ ) and film compressibility ( $\kappa$ ) of TLFs at different temperatures (20 and 34°C) and compression rates (0.15 and 15 A%/s), with the pure water subphase. (c and d) The  $\pi_{\max}$  and  $\kappa$  of TLFs at the physiologically relevant conditions (34°C and 15 A%/s compression rate) in the presence of various subphases. \* $p < 0.05$  indicates statistically significant differences.

PAHSA and BO:CO (Fig. 3 b and d), lysozyme significantly increases the surface pressure. In comparison with the TLF-free control (Fig. 3 f), the influence of lysozyme on PAHSA and BO:CO must be due to adsorption of lysozyme at the air-water surface, thus dominating the surface activity of these two less surface active TLFs.

Statistical analyses of the effect of subphase on the TLFs under the physiologically relevant conditions of 34°C and high compression rate are summarized in Fig. 4 c and d, which shows the  $\pi_{\max}$  and  $\kappa$ , respectively. As shown in Fig. 4 c, the three PC-containing TLFs, i.e., PC, PC:PAHSA, and BO:CO:PC:PAHSA, are all capable of reaching a  $\pi_{\max}$  around 50 mN/m regardless of the subphase. However, the subphase significantly affects the two lipid films without PC, i.e., BO:CO and PAHSA. The  $\pi_{\max}$  of these two TLFs increases with increasing chemical complexity of the subphase. Although the surface pressure increase of BO:CO with lysozyme may be easily explained by the adsorption of this protein to the air-water surface, as also found in previous studies (33,39,60), the case of PAHSA with lysozyme appears to be more complicated. The  $\pi_{\max}$  of PAHSA increases from 30 to 40 mN/m when the subphase is changed from pure water to 1 mM lysozyme. Since the  $\pi_{\max}$  of lysozyme alone is only 34 mN/m (Fig. 3 f), these results must indicate certain synergetic effect or molecular recognition between PAHSA at the surface and lysozyme in the subphase. Similar effects of molecular interactions are also revealed by the  $\kappa$ . As shown in Fig. 4 d,  $\kappa$  of PAHSA increases from 1.7 to 2.5 m/mN with lysozyme in the subphase. Consequently,  $\kappa$  of the TFL increases from 1.4 to 2.3 m/mN, indicating a significant increase in softness.

### Surface rheological properties of the tear lipid films

Fig. 5 a and b shows the elastic ( $E_r$ ) and viscous ( $E_i$ ) moduli of four TLFs, i.e., PC, PAHSA, PC:PAHSA, and BO:CO:PC:PAHSA. All surface dilational moduli were determined at a characteristic surface pressure of 20 mN/m at 34°C, using pure water as the subphase, under a series of frequencies of 0.025, 0.05, 0.1, 0.25, 0.5, and 1 Hz. Given the average duration of each blink for 0.1–0.3 s, the oscillation frequency of 1 Hz is of physiological relevance. The nonpolar lipid film, i.e., BO:CO, was not studied since it does not reach the characteristic surface pressure of 20 mN/m. The procedure of determining the surface dilational moduli can be found in Fig. S4. Fig. S5 demonstrates the accuracy of CDS in determining the surface dilational moduli by comparing to literature values of the DPPC monolayer obtained with the traditional oscillating pendant drop method.

It is found that the  $E_r$  of all TLFs at all frequencies is significantly larger than their  $E_i$ , indicating that all TLFs are more elastic than viscous. The  $E_r$  of all TLFs increases slightly with frequency. The  $E_r$  of PC is almost twice that of PAHSA (90 versus 50 mN/m). Addition of nonpolar lipids, i.e., BO:CO, significantly decreases the  $E_r$  of the TFL. The  $E_r$  of PAHSA and BO:CO:PC:PAHSA is close at the physiologically relevant frequency of 1 Hz.

The  $E_i$  of all TLFs at all frequencies is less than 15 mN/m, except for PC at a very low frequency of 0.025 Hz. The  $E_i$  of PC decreases to a value of 3 mN/m at 1 Hz. In comparison, the  $E_i$  of PAHSA and PC:PAHSA is relatively independent

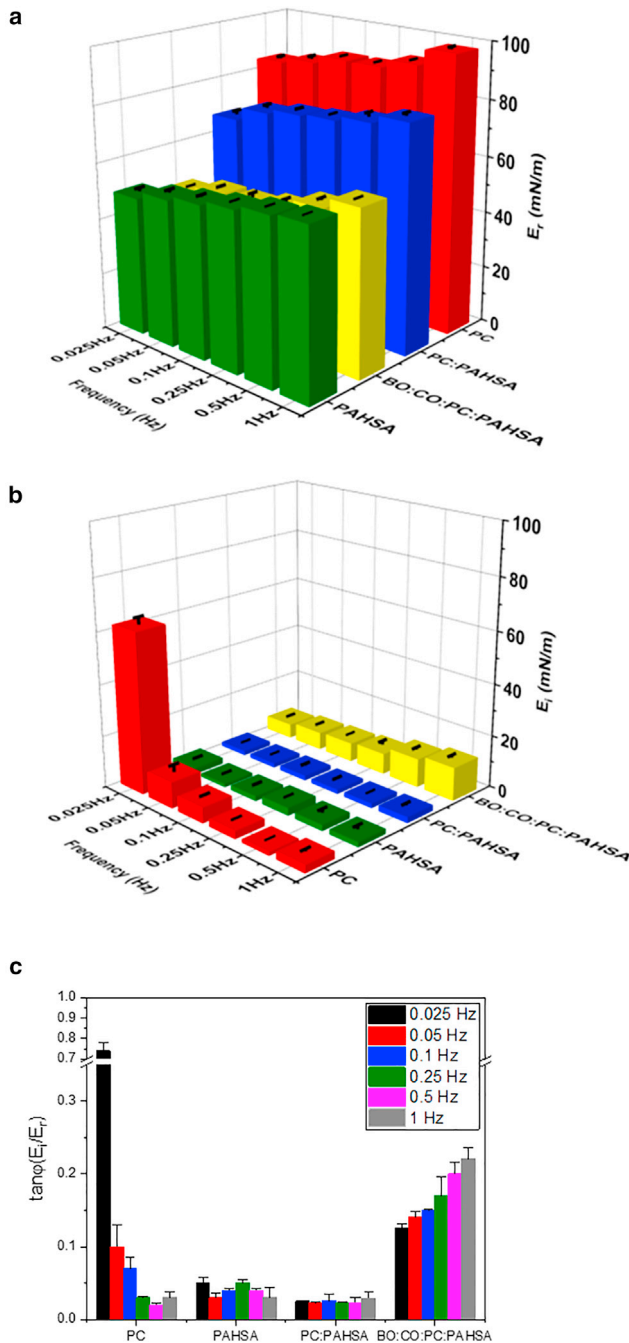


FIGURE 5 Interfacial dilational rheological properties of tear lipid films (TLFs). (a) Elastic ( $E_r$ ) and (b) viscous ( $E_i$ ) surface dilational moduli, and (c) the loss tangent ( $\tan\phi$ ) of PC, PAHSA, PC: PAHSA (3:1), and BO:CO:PC:PAHSA (40:40:15:5), at frequencies of 0.025, 0.05, 0.1, 0.25, 0.5, and 1 Hz. All interfacial rheological properties were determined at the characteristic surface pressure of 20 mN/m and 34°C.

from the oscillation frequency and maintains a low value less than 3 mN/m for all studied frequencies. The  $E_i$  of BO:CO:PC:PAHSA, on the other hand, increases slightly with increasing frequency, to approximately 13 mN/m at the physiologically relevant frequency of 1 Hz.

Fig. 5 c shows the tangent of loss angle, also known as the loss tangent ( $\tan\phi$ ), as a function of the oscillation frequency. In general, the  $\tan\phi$  of PC decreases with increasing frequency and reaches a value less than 0.05 when the oscillation frequency is higher than 0.25 Hz. In comparison, the  $\tan\phi$  of PAHSA and PC:PAHSA is relatively insensitive to the frequency and remains at a low value less than 0.05 at all tested frequencies. The addition of nonpolar lipids, i.e., BO:CO, into the artificial TFL significantly increases the  $\tan\phi$  to above 0.1, indicating a more viscous film than those without the nonpolar lipids. Interestingly, the addition of nonpolar lipids not only increases the  $\tan\phi$  of the TFL but also changes its frequency dependency. It is found that the  $\tan\phi$  of BO:CO:PC:PAHSA increases with the oscillation frequency and reaches a value larger than 0.2 at the physiologically relevant frequency of 1 Hz.

### DISCUSSION

The major physiological function of the TFL is to stabilize the tear film by reducing surface tension and retarding evaporation of the aqueous layer (16,61). However, the specific surface active components of the TFL are still under investigation. Our biophysical studies found that a model TFL that consists of BO:CO:PC:PAHSA (40:40:15:5) is capable of reaching a surface pressure as high as 50 mN/m under physiologically relevant conditions (Fig. 2). This surface pressure corresponds to a surface tension of 20 mN/m, which is much lower than the surface tension of whole tears, reported to be around 43–46 mN/m (36,56,62). In addition, we found that these surface tension values of whole tears reported in literatures are in line with the surface tension of major proteins in the tear aqueous layer, such as lysozyme (Fig. 3). Our study therefore suggested that the static surface tension of whole tears determined in previous studies mostly reflect the equilibrium surface tension of soluble proteins in the tear (63) rather than the dynamic surface tension of the TFL. Being an insoluble lipid film, the TFL is capable of reducing the surface tension significantly lower than that of the whole tears when the TFL is compressed during a blink (14).

It should be noted that the chemical composition of the actual tear aqueous layer is substantially more complicated than that studied here. First, nearly 2000 proteins have been identified in human tears, in which lysozyme, lipocalin, lactoferrin, and secretory immunoglobulin A are known to be the major tear proteins (64,65). Second, tear film contains divalent cations, such as calcium and magnesium, which are known to enhance the stability of the TFL. In vitro experiments using Langmuir trough showed that removing divalent cations from rabbit tears decreased the maximum surface pressure (66). However, the divalent cations were found to have little effect on human tears, likely because the normal osmolarity of rabbit tears is significantly higher than that of humans (66). Third, the pH values of PBS and

Milli-Q water used in this study were 7.4 and 7.0, respectively. The pH value of human tears was reported in the range of 6.8–8.2 (67), with 7.3–7.5 commonly reported for healthy humans (68). This slightly alkaline environment of the tear film affects ionization of fatty acids and gives OAHFAs and PAHSA a negative charge, which is important for their surface activities (1).

Using recombinant lipid films, we have studied the composition-function correlation of the individual lipid components in the TFLL. Our study suggests that phospholipids are most likely to be the primary components responsible for reducing the surface tension of the TFLL (Figs. 2, 3, and 4). The minimum surface tension of the TFLL is close to the equilibrium surface tension ( $\gamma_e$ ) of PC after de novo adsorption at the air-water surface (69). Since the artificial TFLL contains only 15% PC, the TFLL must reach the  $\gamma_e$  of PC by selectively removing other lipids during the highly dynamic process of film compression caused by a blink. Such a process is called “squeeze-out,” likely similar to the biophysical mechanism by which pulmonary surfactant films reduce the surface tension during respiration (43,51,70).

Most interestingly, we found that the major biophysical function of another polar lipid in the artificial TFLL, PAHSA, is not to reduce the surface tension but to optimize the interfacial dilational rheology of the TFLL. When a monolayer that consists of a mixture of lipids is compressed, the maximum surface pressure that the monolayer can sustain, i.e., its collapse pressure, depends on the lipid component with the highest collapse pressure (71). The maximum surface pressure of PAHSA is only 30 mN/m, which is significantly lower than that of PC. Hence, it is unlikely that PAHSA contributes to the biophysical function of TFLL by reducing its surface tension.

Dilational rheological studies provide knowledge about the viscoelastic properties of the TFLL (14). At the physiologically relevant conditions and frequency of 1 Hz, we have measured the elastic ( $E_r$ ) and viscous ( $E_i$ ) moduli of the TFLL to be 58 and 13 mN/m, respectively (Fig. 5). These dilational rheological data are in good agreement with those reported by Raju et al. (72). Using a pendant drop method, these workers have determined the  $E_r$  and  $E_i$  of human meibomian lipid films at 37°C to be approximately 40 and 10 mN/m, respectively. Therefore, our study confirms that the TFLL is overwhelmingly more elastic than viscous under physiologically relevant conditions (62,72,73).

More importantly, using recombinant lipid films, we have found that there are distinct differences in the viscoelastic properties between the two polar lipid components in the artificial TFLL, i.e., PC and PAHSA. One striking difference between these two polar lipids is that the  $E_i$  of PC decreases significantly with increasing frequency, especially in the low frequency range. But the  $E_i$  of PAHSA is relatively independent of the oscillation frequency and maintains a low value for all studied frequencies. Our dilational rheological

measurements of PC are in general agreement with those reported by Wüstneck et al. (74). Using captive bubble surfactometry, these workers found that the  $E_r$  of dipalmitoyl phosphatidylcholine (DPPC) with 2 mol% surfactant protein C was relatively independent of the frequency, but its  $E_i$  decreases significantly with increasing frequency, especially in the low frequency range. In contrast, we found that not only does PAHSA alone demonstrate a low  $E_i$  in a large range of oscillation frequencies, addition of PAHSA, even at a small amount, such as in PC:PAHSA (3:1) and BO:CO:PC:PAHSA (40:40:15:5), is able to significantly reduce the viscosity of the mixed lipid films for all tested frequencies (Fig. 5 b).

This unique property of PAHSA to damp down the viscosity of lipid films and thus to minimize energy dissipation during highly dynamic film oscillation is most likely attributed to its unique molecular structure (Table 1). Both PAHSA and OAHFAs belong to the general lipid class of FAHFAs, which are lipids with potent antidiabetic and anti-inflammatory activities (75,76). OAHFAs differ from the other FAHFAs in that their hydroxy fatty acid backbones are ultralong, typically around 26–34 carbons in length, and their hydroxy esterification is believed to be solely at the terminal ( $\omega$ -) position (31). Being a palmitic acid (C16:0) ester of 9-hydroxy stearic acid (C18:0), the hydroxy fatty acid backbone of PAHSA is much shorter than that of OAHFAs. In addition, PAHSA lacks the acyl chain unsaturation in OAHFAs since oleic acid (C18:1) has been identified as the most abundant acyl chain in OAHFAs of the human TFLL (77). In spite of these differences, PAHSA and OAHFAs share critical structural similarity that predominates their surface activities. Namely, both PAHSA and OAHFAs maintain their amphiphilicity through two hydrophilic moieties favoring contact with water, i.e., a relatively strong contact point through the negatively charged carboxyl group and a relatively weak contact point via the polar ester group. Consequently, PAHSA appears to be a plausible model to understand the biophysical properties of FAHFAs in general and of OAHFAs specifically, to a reasonable extent.

In contrast to phospholipid molecules, which have only one hydrophilic moiety (i.e., their phosphate headgroups), the unique structure of PAHSA molecules enables a new degree of rotational freedom when the lipid film is compressed. In other words, upon highly dynamic compression, the PAHSA molecules at the air-water surface may be able to fold and/or rotate with either one or both hydrophilic moieties in contact with water, depending on the surface area available to the PAHSA molecules. Such intramolecular folding and/or rotation, in spite of not significantly increasing the surface activity, make PAHSA much more efficient than PC in storing the kinetic energy of lateral compression, thus rendering a highly elastic film. We have explored the molecular biophysical mechanism of PAHSA in a companion paper (78).

Similar conclusions can be drawn by examining the loss tangent ( $\tan\phi$ ), which is the ratio between the viscous and the elastic moduli. A perfect elastic material, such as most metals, has a near-zero loss tangent (79). We found that different from PC, which has a very high loss tangent at low frequencies, PAHSA maintains a low loss tangent less than 0.05 for all tested frequencies. Addition of PAHSA to PC, i.e., PC:PAHSA (3:1), decreases its loss tangent from  $\sim 0.7$  to  $\sim 0.03$  at the frequency of 0.025 Hz. The unique viscoelastic property of PAHSA makes the film behave as an elastic solid. This property of PAHSA, likely also that of OAHFAs, is of particular benefit for the TFL since it contains a large portion ( $\sim 80\%$ ) of highly viscous, nonpolar lipids, such as BO and CO, with melting points significantly higher than those of the polar lipids in the TFL (Table 1). It can be seen that the addition of only 5% PAHSA helps maintain the loss tangent of the TFL at a value not much higher than 0.2 (Fig. 5 c). It should be noted that the elasticity of the artificial TFL is significantly higher than that of natural pulmonary surfactant films. The loss tangent of natural pulmonary surfactants, which consist of mostly phospholipids without PAHSA, was found to be approximately 0.4, determined under similar experimental conditions (51). This comparison highlights the importance of OAHFAs in optimizing the rheological properties of the TFL. It is known that the viscosity of TFL of patients with meibomian gland dysfunction increases (14,73,80), whereas the level of OAHFAs in dry eye decreases (81).

## CONCLUSIONS

By studying surface and dilational rheological properties of recombinant lipid films under physiologically relevant conditions, we have studied the composition-function correlations of an artificial TFL that consists of BO:CO:PC:PAHSA (40:40:15:5). We have concluded that the major biophysical function of phospholipids in the TFL is to reduce the surface tension, whereas the primary function of PAHSA is to regulate interfacial rheology of the TFL, thus optimizing the viscoelastic properties of the TFL under physiologically relevant conditions. These findings have novel implications in better understanding the physiological and biophysical functions of the TFL and may offer new translational insight to the treatment of DED.

## SUPPORTING MATERIAL

Supporting material can be found online at <https://doi.org/10.1016/j.bpj.2021.12.033>.

## AUTHOR CONTRIBUTIONS

X.X. and G.L. carried out the experiments and data analysis. Y.Y.Z. designed the research and oversaw the experiments and analysis. Y.Y.Z. and X.X. wrote the paper. All authors discussed the results.

## ACKNOWLEDGMENTS

This research was supported by the National Science Foundation grant number CBET-2011317 (to Y.Y.Z.) and the Mary & Paul Wagner Blindness Prevention Fund of the Hawaii Community Foundation grant number 20ADVC-102168 (to Y.Y.Z.).

## REFERENCES

1. Butovich, I. A. 2013. Tear film lipids. *Exp. Eye Res.* 117:4–27.
2. Cwiklik, L. 2016. Tear film lipid layer: a molecular level view. *Biochim. Biophys. Acta.* 1858:2421–2430.
3. Creech, J., L. T. Do, ..., C. Radke. 1998. In vivo tear-film thickness determination and implications for tear-film stability. *Curr. Eye Res.* 17:1058–1066.
4. McCulley, J., and W. Shine. 1997. A compositional based model for the tear film lipid layer. *Trans. Am. Ophthalmol. Soc.* 95:79.
5. Davidson, H. J., and V. J. Kuonen. 2004. The tear film and ocular mucins. *Vet. Ophthalmol.* 7:71–77.
6. King-Smith, P. E., B. A. Fink, ..., J. M. Tiffany. 2004. The thickness of the tear film. *Curr. Eye Res.* 29:357–368.
7. King-Smith, P. E., E. A. Hinel, and J. J. Nichols. 2010. Application of a novel interferometric method to investigate the relation between lipid layer thickness and tear film thinning. *Cornea.* 51:2418–2423.
8. Chen, J., K. B. Green-Church, and K. K. Nichols. 2010. Shotgun lipidomic analysis of human meibomian gland secretions with electrospray ionization tandem mass spectrometry. *Invest. Ophthalmol. Vis. Sci.* 51:6220–6231.
9. Brown, S. H. J., C. M. E. Kunnen, ..., T. W. Mitchell. 2013. A comparison of patient matched meibum and tear lipidomes. *Cornea.* 54:7417–7423.
10. Butovich, I. A. 2009. The meibomian puzzle: combining pieces together. *Prog. Retin. Eye Res.* 28:483–498.
11. Butovich, I. A. 2011. Lipidomics of human meibomian gland secretions: chemistry, biophysics, and physiological role of meibomian lipids. *Prog. Lipid Res.* 50:278–301.
12. Butovich, I. A., J. C. Wojtowicz, and M. Molai. 2009. Human tear film and meibum. Very long chain wax esters and (O-acyl)-omega-hydroxy fatty acids of meibum. *J. Lipid Res.* 50:2471–2485.
13. Chen, J., K. B. Green, and K. K. Nichols. 2013. Quantitative profiling of major neutral lipid classes in human meibum by direct infusion electrospray ionization mass spectrometry. *Invest. Ophthalmol. Vis. Sci.* 54:5730–5753.
14. Georgiev, G. A., P. Eftimov, and N. Yokoi. 2017. Structure-function relationship of tear film lipid layer: a contemporary perspective. *Exp. Eye Res.* 163:17–28.
15. Millar, T. J., and B. S. Schuett. 2015. The real reason for having a meibomian lipid layer covering the outer surface of the tear film - a review. *Exp. Eye Res.* 137:125–138.
16. Bron, A., J. Tiffany, ..., L. Voon. 2004. Functional aspects of the tear film lipid layer. *Exp. Eye Res.* 78:347–360.
17. Behrens, A., and J. J. Doyle. 2006. Dysfunctional tear syndrome. *Cornea.* 25:900–907.
18. Milner, M. S., K. A. Beckman, ..., E. Yeu. 2017. Dysfunctional tear syndrome: dry eye disease and associated tear film disorders – new strategies for diagnosis and treatment. *Curr. Opin. Ophthalmol.* 28:3–47.
19. Stapleton, F., M. Alves, ..., L. Jones. 2017. TFOS DEWS II epidemiology report. *Ocul. Surf.* 15:334–365.
20. Pflugfelder, S. C., A. Solomon, and M. E. Stern. 2000. The diagnosis and management of dry eye: a twenty-five-year review. *Cornea.* 19:644–649.
21. Lemp, M. A., and G. N. Foulks. 2007. The definition and classification of dry eye disease. *Ocul. Surf.* 5:75–92.

22. Jones, L., L. E. Downie, ..., J. P. Craig. 2017. TFOS DEWS II management and therapy report. *Ocul. Surf.* 15:575–628.
23. Yu, J., C. V. Asche, and C. J. Fairchild. 2011. The economic burden of dry eye disease in the United States: a decision tree analysis. *Cornea.* 30:379–387.
24. Kulovesi, P., A. H. Rantamäki, and J. M. Holopainen. 2014. Surface properties of artificial tear film lipid layers: effects of wax esters. *Invest. Ophthalmol. Vis. Sci.* 55:4448.
25. Kulovesi, P., J. Telenius, ..., J. M. Holopainen. 2012. The impact of lipid composition on the stability of the tear fluid lipid layer. *Soft Matter.* 8:5826–5834.
26. Kulovesi, P., J. Telenius, ..., I. Vattulainen. 2010. Molecular organization of the tear fluid lipid layer. *Biophys. J.* 99:2559–2567.
27. Butovich, I. A., J. C. Arciniega, and J. C. Wojtowicz. 2010. Meibomian lipid films and the impact of temperature. *Invest. Ophthalmol. Vis. Sci.* 51:5508–5518.
28. Leiske, D. L., S. R. Raju, ..., G. G. Fuller. 2010. The interfacial viscoelastic properties and structures of human and animal meibomian lipids. *Exp. Eye Res.* 90:598–604.
29. Dwivedi, M., M. Brinkkotter, ..., H. J. Galla. 2014. Biophysical investigations of the structure and function of the tear fluid lipid layers and the effect of ectoine. Part B: artificial lipid films. *Biochim. Biophys. Acta.* 1838:2716–2727.
30. Lam, S. M., L. Tong, ..., G. Shui. 2014. Extensive characterization of human tear fluid collected using different techniques unravels the presence of novel lipid amphiphiles. *J. Lipid Res.* 55:289–298.
31. Hancock, S. E., R. Ailuri, ..., S. J. Blanksby. 2018. Mass spectrometry-directed structure elucidation and total synthesis of ultra-long chain (O-acyl)- $\omega$ -hydroxy fatty acids. *J. Lipid Res.* 59:1510–1518.
32. Tragoulias, S. T., P. J. Anderton, ..., T. J. Millar. 2005. Surface pressure measurements of human tears and individual tear film components indicate that proteins are major contributors to the surface pressure. *Cornea.* 24:189–200.
33. Mudgil, P., M. Torres, and T. J. Millar. 2006. Adsorption of lysozyme to phospholipid and meibomian lipid monolayer films. *Colloids Surf. B Biointerfaces.* 48:128–137.
34. Mudgil, P., and T. J. Millar. 2011. Surfactant properties of human meibomian lipids. *Invest. Ophthalmol. Vis. Sci.* 52:1661–1670.
35. Saaren-Seppälä, H., M. Jauhiainen, ..., J. M. Holopainen. 2005. Interaction of purified tear lipocalin with lipid membranes. *Invest. Ophthalmol. Vis. Sci.* 46:3649–3656.
36. Tiffany, J. M., N. Winter, and G. Bliss. 1989. Tear film stability and tear surface tension. *Curr. Eye Res.* 8:507–515.
37. Miano, F., M. Calcarà, ..., V. Enea. 2005. Insertion of tear proteins into a meibomian lipids film. *Colloids Surf. B Biointerfaces.* 44:49–55.
38. Holly, F. J., J. T. Patten, and C. H. Dohlman. 1977. Surface activity determination of aqueous tear components in dry eye patients and normals. *Exp. Eye Res.* 24:479–491.
39. Svitova, T. F., and M. C. Lin. 2010. Tear lipids interfacial rheology: effect of lysozyme and lens care solutions. *Optom. Vis. Sci.* 87:10.
40. Purslow, C., and J. S. Wolffsohn. 2005. Ocular surface temperature: a review. *Eye Contact Lens.* 31:117–123.
41. Ousler, G. W., 3rd, M. B. Abelson, ..., L. M. Smith. 2014. Blink patterns and lid-contact times in dry-eye and normal subjects. *Clin. Ophthalmol.* 8:869–874.
42. Cardona, G., C. Garcia, ..., J. Gispets. 2011. Blink rate, blink amplitude, and tear film integrity during dynamic visual display terminal tasks. *Curr. Eye Res.* 36:190–197.
43. Zuo, Y. Y., R. A. Veldhuizen, ..., F. Possmayer. 2008. Current perspectives in pulmonary surfactant—inhibition, enhancement and evaluation. *Biochim. Biophys. Acta.* 1778:1947–1977.
44. Dartt, D. A. 2011. Tear lipocalin: structure and function. *Ocul. Surf.* 9:126–138.
45. Wizert, A., D. R. Iskander, and L. Cwiklik. 2017. Interaction of lysozyme with a tear film lipid layer model: a molecular dynamics simulation study. *Biochim. Biophys. Acta Biomembr.* 1859:2289–2296.
46. Flanagan, J. L., and M. D. P. Willcox. 2009. Role of lactoferrin in the tear film. *Biochimie.* 91:35–43.
47. Valle, R. P., W. Tony, and Y. Y. Zuo. 2015. Biophysical influence of airborne carbon nanomaterials on natural pulmonary surfactant. *ACS Nano.* 9:5413–5421.
48. Zuo, Y. Y., R. Chen, ..., A. W. Neumann. 2016. Phase transitions in dipalmitoylphosphatidylcholine monolayers. *Langmuir.* 32:8501–8506.
49. Yang, Y., Y. Wu, ..., Y. Y. Zuo. 2018. Biophysical assessment of pulmonary surfactant predicts the lung toxicity of nanomaterials. *Small Methods.* 2:1700367.
50. Yang, Y., L. Xu, ..., Y. Y. Zuo. 2018. Aggregation state of metal-based nanomaterials at the pulmonary surfactant film determines biophysical inhibition. *Environ. Sci. Technol.* 52:8920–8929.
51. Xu, L., Y. Yang, and Y. Y. Zuo. 2020. Atomic force microscopy imaging of adsorbed pulmonary surfactant films. *Biophys. J.* 119:756–766.
52. Rantamäki, A. H., J. Telenius, ..., J. M. Holopainen. 2011. Lessons from the biophysics of interfaces: lung surfactant and tear fluid. *Prog. Retin. Eye Res.* 30:204–215.
53. Butovich, I. A., T. J. Millar, and B. M. Ham. 2008. Understanding and analyzing meibomian lipids—a review. *Curr. Eye Res.* 33:405–420.
54. Lu, H., J. C. Wojtowicz, and I. A. Butovich. 2013. Differential scanning calorimetric evaluation of human meibomian gland secretions and model lipid mixtures: transition temperatures and cooperativity of melting. *Chem. Phys. Lipids.* 170-171:55–64.
55. Yu, K., J. Yang, and Y. Y. Zuo. 2016. Automated droplet manipulation using closed-loop axisymmetric drop shape analysis. *Langmuir.* 32:4820–4826.
56. Tiffany, J. M. 2006. Surface tension in tears. *Arch. Soc. Esp. Ophthalmol.* 81:363–366.
57. Braun, R. J. 2012. Dynamics of the tear film. *Annu. Rev. Fluid Mech.* 44:267–297.
58. Yu, K., J. Yang, and Y. Y. Zuo. 2018. Droplet oscillation as an arbitrary waveform generator. *Langmuir.* 34:7042–7047.
59. Yang, J., K. Yu, ..., Y. Y. Zuo. 2019. Determining the surface dilational rheology of surfactant and protein films with a droplet waveform generator. *J. Colloid Interface Sci.* 537:547–553.
60. Nishimura, S. Y., G. M. Magana, ..., G. G. Fuller. 2008. Effect of lysozyme adsorption on the interfacial rheology of DPPC and cholesteryl myristate films. *Langmuir.* 24:11728–11733.
61. Svitova, T. F., and M. C. Lin. 2021. Evaporation retardation by model tear-lipid films: the roles of film aging, compositions and interfacial rheological properties. *Colloids Surf. B Biointerfaces.* 197:111392.
62. Svitova, T. F., and M. C. Lin. 2016. Dynamic interfacial properties of human tear-lipid films and their interactions with model-tear proteins in vitro. *Adv. Colloid Interface Sci.* 233:4–24.
63. Nagyova, B., and J. Tiffany. 1999. Components responsible for the surface tension of human tears. *Curr. Eye Res.* 19:4–11.
64. Willcox, M. D. 2019. Tear film, contact lenses and tear biomarkers. *Clin. Exp. Optom.* 102:350–363.
65. Zhou, L., S. Z. Zhao, ..., R. W. Beuerman. 2012. In-depth analysis of the human tear proteome. *J. Proteomics.* 75:3877–3885.
66. Wei, X. E., M. Markoulli, ..., Z. Zhao. 2012. Divalent cations in tears, and their influence on tear film stability in humans and rabbits. *Invest. Ophthalmol. Vis. Sci.* 53:3280–3285.
67. Willcox, M. D. P., P. Argueso, ..., L. Jones. 2017. TFOS DEWS II tear film report. *Ocul. Surf.* 15:366–403.
68. Yamada, M., H. Mochizuki, ..., Y. Mashima. 1997. Fluorophotometric measurement of pH of human tears in vivo. *Curr. Eye Res.* 16:482–486.
69. Bai, X., L. Xu, ..., G. Hu. 2019. Adsorption of phospholipids at the air-water surface. *Biophys. J.* 117:1224–1233.

70. Keating, E., Y. Y. Zuo, ..., R. A. Veldhuizen. 2012. A modified squeeze-out mechanism for generating high surface pressures with pulmonary surfactant. *Biochim. Biophys. Acta.* 1818:1225–1234.
71. Lee, K. Y. 2008. Collapse mechanisms of Langmuir monolayers. *Annu. Rev. Phys. Chem.* 59:771–791.
72. Raju, S. R., C. K. Palaniappan, ..., T. J. Millar. 2013. Interfacial dilatational viscoelasticity of human meibomian lipid films. *Curr. Eye Res.* 38:817–824.
73. Georgiev, G. A., N. Yokoi, ..., R. Krastev. 2014. Surface relaxations as a tool to distinguish the dynamic interfacial properties of films formed by normal and diseased meibomian lipids. *Soft Matter.* 10:5579–5588.
74. Wüstneck, N., R. Wüstneck, ..., U. Pison. 2001. Interfacial behaviour and mechanical properties of spread lung surfactant protein/lipid layers. *Colloids Surf. B Biointerfaces.* 21:191–205.
75. Yore, M. M., I. Syed, ..., B. B. Kahn. 2014. Discovery of a class of endogenous mammalian lipids with anti-diabetic and anti-inflammatory effects. *Cell.* 159:318–332.
76. Nelson, A. T., M. J. Kolar, ..., D. Siegel. 2017. Stereochemistry of endogenous palmitic acid ester of 9-hydroxystearic acid and relevance of absolute configuration to regulation. *J. Am. Chem. Soc.* 139:4943–4947.
77. Butovich, I. 2010. Biochemistry and biophysics of human and animal tear film lipid layer: from composition to structure to function. *Invest. Ophthalmol. Vis. Sci.* 51:4154.
78. Xu, X., K. Kang, ..., Y. Y. Zuo. 2021. Biophysical properties of tear film lipid layer II. Polymorphism of FAHFA. *Biophys. J.*, Submitted as a companion paper.
79. Miller, R., J. K. Ferri, ..., R. Wüstneck. 2010. Rheology of interfacial layers. *Colloid Polym. Sci.* 288:937–950.
80. Svitova, T. F., and M. C. Lin. 2013. Racial variations in interfacial behavior of lipids extracted from worn soft contact lenses. *Optom. Vis. Sci.* 90:1361–1369.
81. Lam, S. M., L. Tong, ..., M. R. Wenk. 2011. Meibum lipid composition in Asians with dry eye disease. *PLoS One.* 6:e24339.